

Exploration of Significant Optical Parameters of Selected Metal Oxide Nanoparticles Using Optical Spectroscopy

J.M. Rami and C.D. Patel

Faculty of Science and Humanities, Sankalchand Patel University, Visnagar, Gujarat, India

*Correspondence to:

J.M. Rami
Faculty of Science and Humanities,
Sankalchand Patel University,
Visnagar, Gujarat, India.
E-mail: jr17792@gmail.com

Received: November 24, 2022

Accepted: May 16, 2023

Published: May 18, 2023

Citation: Rami JM, Patel CD. 2023. Exploration of Significant Optical Parameters of Selected Metal Oxide Nanoparticles Using Optical Spectroscopy. *NanoWorld J* 9(S1): S601-S605.

Copyright: © 2023 Rami and Patel. This is an Open Access article distributed under the terms of the Creative Commons Attribution 4.0 International License (CCBY) (<http://creativecommons.org/licenses/by/4.0/>) which permits commercial use, including reproduction, adaptation, and distribution of the article provided the original author and source are credited.

Published by United Scientific Group

Abstract

This investigation involved the synthesis and optical characterization of Copper Oxide (CuO), Cobalt Oxide (Co₂O₃), Iron Oxide (Fe₂O₃), and Zinc oxide (ZnO) nanoparticles carried out by UV-Vis (Ultraviolet-Visible) Spectroscopy. UV-Vis spectra of nanoparticles were performed on a Perkin-Elmer Lambda-19 UV-Vis spectrometer. The absorption co-efficient dependent on energy was deliberated by the Tauc method and energy bandgap of nanoparticles were measured using UV-Vis spectra and compared with reported samples. Important optical variables such as refractive index, extinction co-efficient, and dielectric constant [real and imaginary parts] were computed for the entire scope of information with a hypothetical basis and detailed in the concern section.

Keywords

Metal oxide nanoparticles, UV-Vis spectra, Refractive index, Extinction co-efficient, Dielectric constant

Introduction

Electrical properties and optical properties of materials at the nanoscale differ from those at the bulk level. Metal oxide nanoparticles are essential among the most used nanomaterials because of their superior electrical, electrochemical, paint/ink materials, catalytic, and magnetic properties. Metal oxide nanoparticles have shown promising results in terms of physical and chemical properties owing to their high density and lesser size [1]; consequently, it is critical to understand their many features in terms of properties and applications. Optical materials are difficult to make from a single crystal and require easy-to-mold environmental protection in nanocomposites. The optical materials have improved characteristics at the nanoscale, and the nanoparticles are held together by a polymer surrounding substance. For a variety of reasons, the electrical characteristics of transition metal oxide alter when they are in the nano-size. For the same volume of fraction, a fall in particle size reduces interparticle distance, inducing percolation and an increase in electrical properties due to quantum processes. Since it is employed for photoconductive and photothermic applications, CuO, a semi-conductor oxide with a bandgap of ~1.21 eV, has gotten more consideration [2]. CuO nanoparticles have a lot of potential in photocatalytic and sensor [3] applications. Due to its use as a photocatalyst [4], extremely discriminating cobalt sensor [5], greater temp. solar discriminating absorber [6], thin film super-capacitors electrode substantial [7], and in electro-chromic devices [8]. Co₂O₃ is notorious as a potential oxide since it changes its photosensitive characteristics in response to an external electrical input. Fe₂O₃ is a low-cost substance that is stable, easy to manufacture, non-toxic, and environmentally friendly. This nanoparticle is thought to be a good fit for a variety of uses, including catalytic-agent, sensor-devices, colorants, data-storage materials, fine ceramics, and photo-electro-

chemical cells [8]. ZnO things are a stimulating material with a large band gap (3.37 eV), a 60 meV excitant binding energy, and remarkable chemical stability [9]. The theoretical investigation of organizational, electrical, photosensitive, and thermo-dynamic features of ZnO materials culminated the experimental interest in the material [10, 11]. ZnO is a viable option for various technical applications. ZnO is a carrying out chemical as a crystal-clear electrical interface for solar cells because of its non-toxicity, availability, and inexpensive cost [12]. Because of its features in a variety of industrial applications, some researchers concentrated their efforts on obtaining high-quality ZnO. ZnO nanoparticles are employed as transparent electrodes with excellent conductivity and little loss of optical transmission.

Materials and Methods

Four commercially available metal oxide nanoparticles of Copper, Cobalt, Iron, and Zinc were used in this paper and prepared by chemical co-precipitation method. All of the compounds are AR grade and employed without being purified further.

For the formation of nanoparticles, freshly formed aqueous solutions of the compounds are employed. Oxide nanoparticles of Copper, Cobalt, Iron, and Zinc are prepared by adding simultaneously the metal oxide solution to the solution of ethylene-diamine-tetra-acetic acid (EDTA) which is vigorously agitated with a magnetic-stirrer. The purpose of the other solution was to stabilize the atoms prior to combination, that is possibly will shrink the particle to smaller particle size. To remove contaminations, including EDTA waste, and to eliminate any original reactant, the carbonates of metal precipitate generated by this reaction are removed from the assortment and splashed several times with filtered water and then with alcohol. To get metal-carbonate precursor in the form of extremely fine powder, the wet precipitate is dried and methodically pulverized with an agate-mortar. The metal-carbonate precursor converts into metal oxide nanoparticles at high temperatures.

In the existing paper UV-Vis absorption spectrum of selected metal oxide nanoparticles was investigated at ambient temperature (200 - 1600 nm wavelength) by Shimadzu, model UV-3600 spectrophotometer in CHARUSAT, Changa, Gujarat and different optical parameters were calculated in concern section.

Results and Discussion

The optical absorption spectra of all metal oxide nanoparticles were noted down by using Perkin-Elmer Lambda-19 UV-VIS-NIR spectrometer. Absorption spectra for all four-metal oxide nanoparticles presented in figure 1. Absorption spectra indicates that nanomaterials are extremely absorptive in wavelength range 200 - 600 nm. In the case of CuO, Co₂O₃, Fe₂O₃, and ZnO nanoparticles strong absorption bands are observed at 270 nm, 210 nm, 435 nm, and 377 nm, respectively, which corresponds to excitation of surface plasmons in the composite nanoparticles [13-16]. This band could be the result of the electromagnetic modes of nearby particles coupling. It

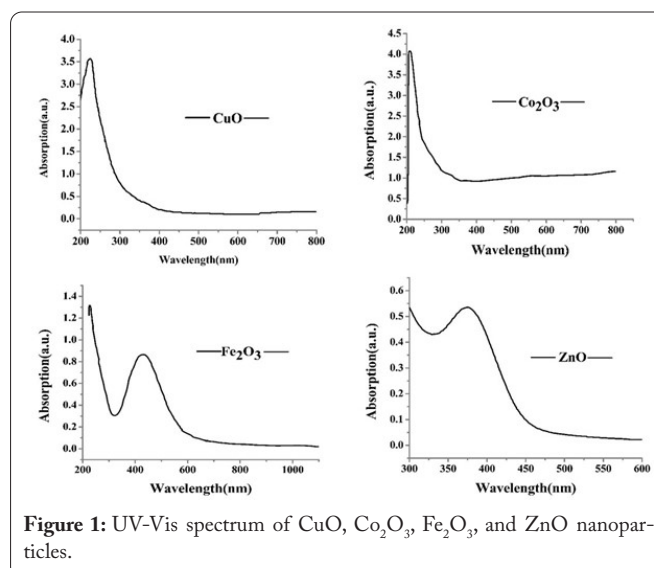


Figure 1: UV-Vis spectrum of CuO, Co₂O₃, Fe₂O₃, and ZnO nanoparticles.

can be seen from the absorption spectra of all the metal oxide nanoparticles that absorption reduces as wavelength increases. The fact that the absorbance has decreased suggests that these metal oxide nanoparticles have an optical bandgap.

Energy bandgap

Photon absorption brought on by an electron transition is used to determine the type and value of the photonic band-gap energy [17]. The value of the absorption co-efficient (α) is affected by both particle emission energy and nanoparticles composition, which is calculated using equation (1).

$$\alpha t = 2.303A \quad (1)$$

Where, 'A' denotes the value of absorbance and 't' indicates the sample's concentration thickness. This basic absorption, which is correlated with the shift of electron, might well be defining the optical gap of the metal oxide nanoparticles.

The co-efficient (α) can be calculated with equation (2), which is typical method for sympathetic the nature of carrier transitions in any form of material [18].

$$\alpha = \frac{(h\nu - E_g)^m}{h\nu} \quad (2)$$

Where, 'h' is a Plank constant and $\nu = c/\lambda$, E_g = band gap and proponent 'm' is rest on the band's dimensionality and nature of transitions.

Tauc relation for Energy band of materials given by,

$$\ln(\alpha h\nu) \text{ vs } \ln(h\nu - E_g) \quad (3)$$

Where, 'm' is having the values 1/2, 3/2, 2 or 3 liable on the nature of the electronic transition accountable for the absorption.

The slop of the graph $\ln(\alpha h\nu) \text{ vs } \ln(h\nu - E_g)$ for CuO, Co₂O₃, Fe₂O₃, and ZnO nanoparticles are shown in figure 2, the value of slope is approximately ~0.5 which indicates the allowed direct nature of transition [19]. Further, the graph of $(\alpha h\nu)^2$ and $h\nu$ in eV provides the precise direct bandgap value.

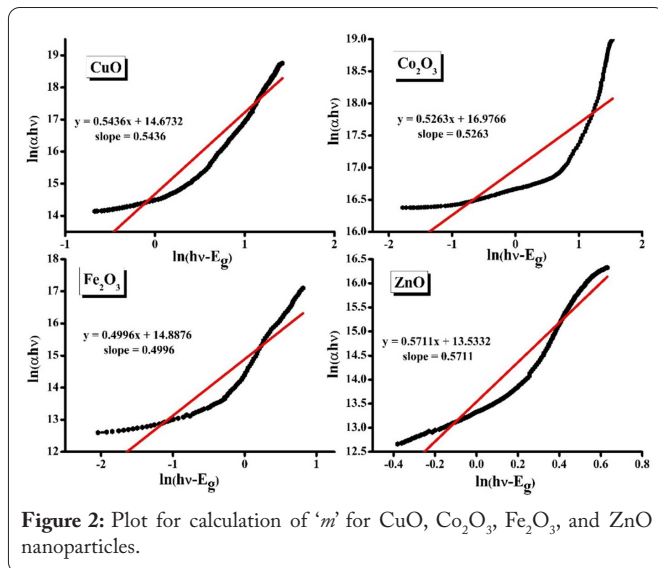


Figure 2: Plot for calculation of 'm' for CuO, Co₂O₃, Fe₂O₃, and ZnO nanoparticles.

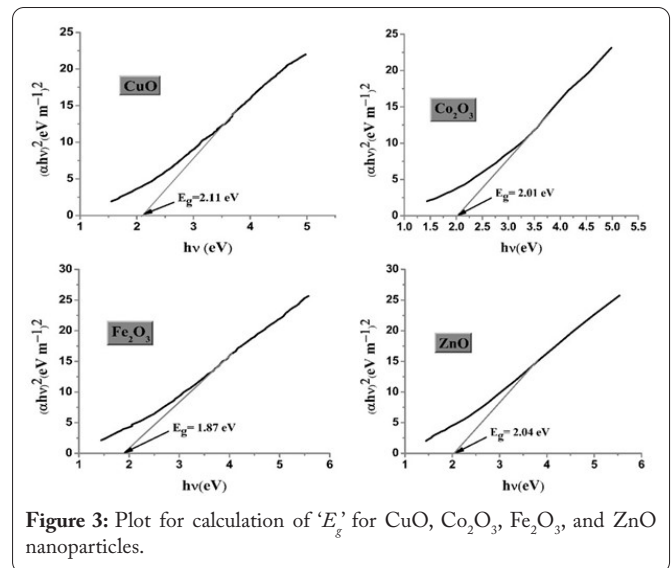


Figure 3: Plot for calculation of 'E_g' for CuO, Co₂O₃, Fe₂O₃, and ZnO nanoparticles.

Distinction of (αhv)² with hv for nanoparticles are shown in below figure 3, where extrapolation of straight line to (αhv)² = 0 gives the metal oxide nanoparticles bandgap values. The value of optical bandgap of selected nanoparticles so obtained are tabulated in table 1. The data obtained is found compatible with the previous recorded data [20-23]. The material requires more energy to shift electrons at nano level. As a result, the bandgap energy of nanoparticles is greater than that of the bulk material.

Optical parameters

The relationship between α and refractive index (η) reveals the polarization of the material through the electromagnetic field of light, could be measured. The fluctuation of linear and non-linear optical characteristics of all metal oxide nanoparticles was explored in order to offer a critical perspective on the non-linear optical parameters of chosen nanoparticles inside ethanol solvent. The refractive index of selected nanoparticles is calculated using the following relationship.

$$\eta = \frac{1+R}{1-R} + \sqrt{\frac{4R}{(1-R)^2} - K^2} \quad (4)$$

Where, R denotes reflectance, η = refractive index, K = α/4π is the extinction co-efficient.

The graph of refractive index and extinction co-efficient were shown in figure 4 and figure 5, respectively.

The medium's optical characteristics are well-defined by a N = η - iK (complex refractive index) and E = E_r - E_i (complex dielectric constant). The real portion E_r often refers to dispersion, whereas the imaginary part E_i offers a measure of the wave's dissipative rate in the medium. The relation which links the real and imaginary components of the di-electric constants to η and K given below.

$$E_r = \eta^2 - K^2$$

$$E_i = 2\eta K$$

The plot of di-electric constant real part (E_r) and imag-

Table 1: Optical bandgap of nanoparticles with obtain transition.

Nanoparticles	Types of bandgap	Conjunction	Bandgap in eV
CuO	Direct	Allowed	2.11
Co ₂ O ₃	Direct	Allowed	2.01
Fe ₂ O ₃	Direct	Allowed	1.87
ZnO	Direct	Allowed	2.04

inary part (E_i) as a function of wavelength for CuO, Co₂O₃, Fe₂O₃, and ZnO nanoparticles depicted in figure 6 and figure 7, respectively.

Conclusions

Transition oxide nanoparticles such as CuO, Co₂O₃, Fe₂O₃, and ZnO prepared using co-precipitation method was deliberate with the UV-Vis spectroscopy method. All absorption spectra for nanoparticles illustrate a significant absorption of occurrence in visible and near IR range of electromagnetic spectrum. CuO, Co₂O₃, Fe₂O₃, and ZnO nanoparticles have been shown to have a direct permitted charge transition due to high absorption. The appraised optical bandgaps nearby

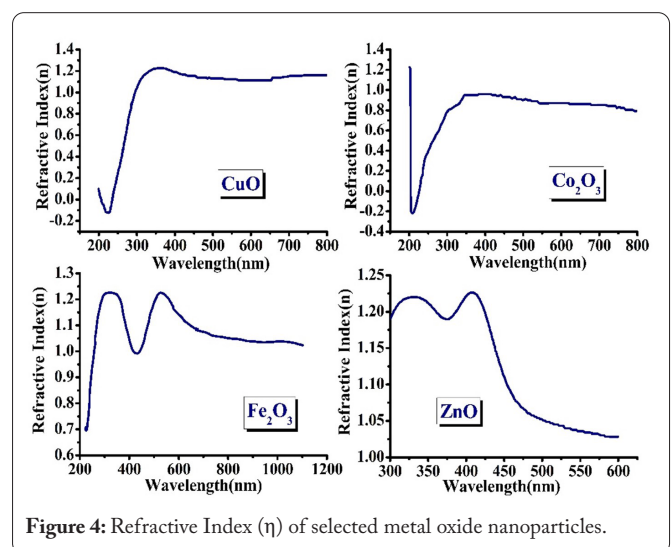


Figure 4: Refractive Index (η) of selected metal oxide nanoparticles.

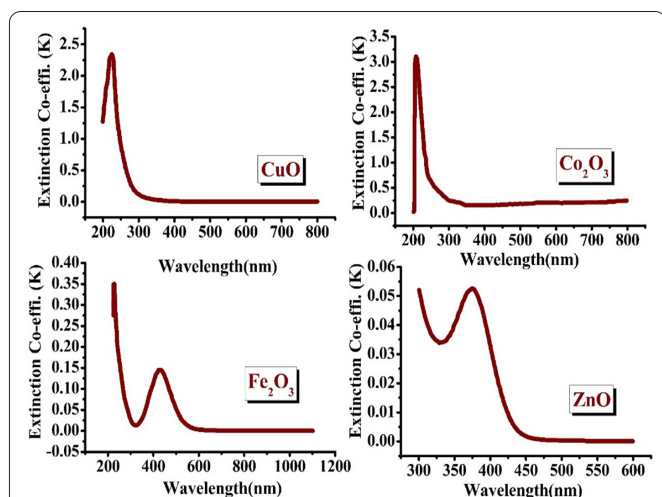


Figure 5: Extinction co-efficient (K) of selected metal oxide nanoparticles.

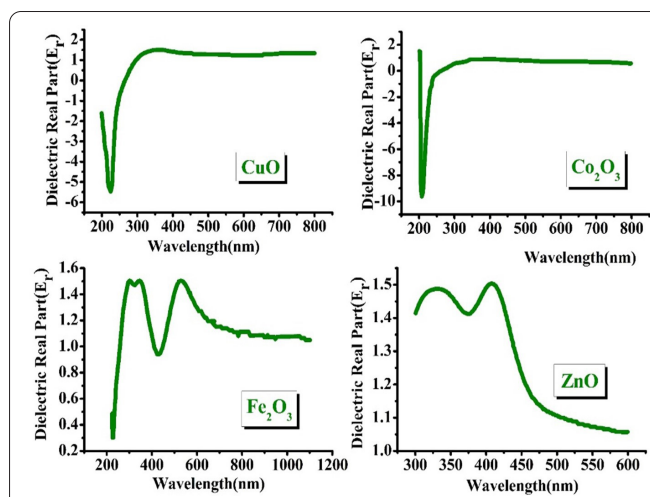


Figure 6: Dielectric real part (E_r) of selected metal oxide nanoparticles.

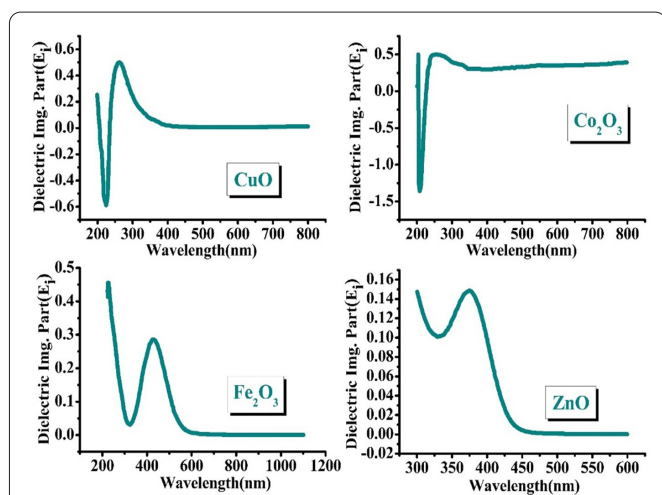


Figure 7: Dielectric imaginary part (E_i) of selected metal oxide nanoparticles.

1.87 to 2.11 eV for all metal oxide nanoparticle are worthy agreement with the experimental values. The refractive index found nearly between 1.0 to 1.3 for all nanoparticles, value of extinction co-efficient is 2.3 for CuO, 3.1 for Co_2O_3 , varies between 0.01 to 0.35 and 0.01 to 0.05 for Fe_2O_3 and ZnO, respectively. The real part of di-electric constant found between 0 to 1 for CuO and Co_2O_3 , while between 1.4 to 1.5 for Fe_2O_3 and ZnO nanoparticles. Imaginary part of di-electric constant found between 0.2 to 0.5 for CuO, Co_2O_3 , and Fe_2O_3 , and it varies between 0.10 to 0.15 for ZnO nanoparticle. The study has publicized that these kinds of nanoparticles can be used to study a variety of material properties, including catalysis, electricity, optical properties, and many others, in the fields of physics, chemistry, and biology. We can also find toxic or non-toxic properties of medicines in medical science.

Acknowledgements

The authors acknowledge the help and inputs of Dr. K.C.Patel R & D Center, CHARUSAT, Changa, Gujarat, India in characterization of selected nanoparticles.

Conflict of Interest

The authors declare that they have no conflict of interests.

Credit Author Statement

J. M. Rami: Conceptualization, Methodology, Investigation, Visualization, Formal analysis, Data curation, Writing - original draft preparation; C. D. Patel: Data validation, Writing - review and editing, Supervision. All the authors read and approved the manuscript.

References

- Link S, El-Sayed MA. 2000. Shape and size dependence of radiative, non-radiative and photothermal properties of gold nanocrystals. *Int Rev Phys Chem* 19(3): 409-453. <https://doi.org/10.1080/01442350050034180>
- Nunes D, Pimentel A, Santos L, Barquinha P, Pereira L, et al. 2019. Structural, optical, and electronic properties of metal oxide nanostructures. *Met Oxide Nanostruct* 59-102.
- Pourbeyram S, Abdollahpour J, Soltanpour M. 2019. Green synthesis of copper oxide nanoparticles decorated reduced graphene oxide for high sensitive detection of glucose. *Mater Sci Eng C* 94: 850-857. <https://doi.org/10.1016/j.msec.2018.10.034>
- Lou X, Han J, Chu W, Wang X, Cheng Q. 2007. Synthesis and photocatalytic property of Co_3O_4 nanorods. *Mater Sci Eng B* 137(1-3): 268-271. <https://doi.org/10.1016/j.mseb.2006.12.002>
- Yamaura H, Tamaki J, Moriya K, Miura N, Yamazoe N. 1997. Highly selective CO sensor using indium oxide doubly promoted by cobalt oxide and gold. *J Electrochem Soc* 144(6): L158. <https://doi.org/10.1149/1.1837710>
- Chidambaram K, Malhotra LK, Chopra KL. 1982. Spray-pyrolysed cobalt black as a high temperature selective absorber. *Thin Solid Films* 87(4): 365-371. [https://doi.org/10.1016/0040-6090\(82\)90289-9](https://doi.org/10.1016/0040-6090(82)90289-9)
- Kim HK, Seong TY, Lim JH, Cho WI, Yoon YS. 2001. Electrochemical and structural properties of radio frequency sputtered cobalt oxide electrodes for thin-film supercapacitors. *J Power Sources* 102(1-2): 167-171. [https://doi.org/10.1016/S0378-7753\(01\)00864-3](https://doi.org/10.1016/S0378-7753(01)00864-3)
- Maruyama T, Arai S. 1996. Electrochromic properties of cobalt oxide thin films prepared by chemical vapor deposition. *J Electrochem Soc* 143(4): 1383. <https://doi.org/10.1149/1.1836646>
- Chen J, Xu L, Li W, Gou X. 2005. $\alpha\text{-Fe}_2\text{O}_3$ nanotubes in gas sensor and lithium-ion battery applications. *Adv Mater* 17(5): 582-586. <https://doi.org/10.1002/adma.200401101>

- Lu F, Cai W, Zhang Y. 2008. ZnO hierarchical micro/nanoarchitectures: solvothermal synthesis and structurally enhanced photocatalytic performance. *Adv Funct Mater* 18(7): 1047-1056. <https://doi.org/10.1002/adfm.200700973>
- Kaddes M, Omri K, Kouaydi N, Zemzemi M. 2018. Structural, electrical and optical properties of ZnO nanoparticle: combined experimental and theoretical study. *Appl Phys A* 124: 518. <https://doi.org/10.1007/s00339-018-1921-x>
- Özgür Ü, Hofstetter D, Morkoc H. 2010. ZnO devices and applications: a review of current status and future prospects. *Proc IEEE* 98(7): 1255-1268. <https://doi.org/10.1109/JPROC.2010.2044550>
- Lanje AS, Sharma SJ, Pode RB, Ningthoujam RS. 2010. Synthesis and optical characterization of copper oxide nanoparticles. *Adv Appl Sci Res* 1(2): 36-40.
- Iravani S, Varma RS. 2020. Sustainable synthesis of cobalt and cobalt oxide nanoparticles and their catalytic and biomedical applications. *Green Chem* 22(9): 2643-2661. <https://doi.org/10.1039/D0GC00885K>
- Ali A, Zafar H, Zia M, ul Haq I, Phull AR, et al. 2016. Synthesis, characterization, applications, and challenges of iron oxide nanoparticles. *Nanotechnol Sci Appl* 9: 49-67. <https://doi.org/10.2147/NSA.S99986>
- Jiang J, Pi J, Cai J. 2018. The advancing of zinc oxide nanoparticles for biomedical applications. *Bioinorg Chem Appl* 2018: 1062562. <https://doi.org/10.1155/2018/1062562>
- Makula P, Pacia M, Macyk W. 2018. How to correctly determine the band gap energy of modified semiconductor photocatalysts based on UV-Vis spectra. *J Phys Chem Lett* 9(23): 6814-6817. <https://doi.org/10.1021/acs.jpcllett.8b02892>
- Bardeen J, Blatt FJ, Hall LH. 1956. In Proceedings of Photoconductivity conference, Atlantic city, New York.
- Dholakia DA, Solanki GK, Patel SG, Agarwal MK. 2003. Optical band gap studies of tungsten sulphoselenide single crystals grown by a DVT technique. *Scientia Iranica* 10(4): 373-382.
- Mukherjee N, Show B, Maji SK, Madhu U, Bhar SK, et al. 2011. CuO nano-whiskers: electrodeposition, Raman analysis, photoluminescence study and photocatalytic activity. *Mater Lett* 65(21-22): 3248-3250. <https://doi.org/10.1016/j.matlet.2011.07.016>
- Zhu X, Wang J, Nguyen D, Thomas J, Norwood RA, et al. 2012. Linear and nonlinear optical properties of Co₃O₄ nanoparticle-doped polyvinyl-alcohol thin films. *Opt Mater Express* 2(1): 103-110. <https://doi.org/10.1364/OME.2.000103>
- Deotale AJ, Nandedkar RV. 2016. Correlation between particle size, strain and band gap of iron oxide nanoparticles. *Mater Today Proc* 3(6): 2069-2076. <https://doi.org/10.1016/j.matpr.2016.04.110>
- Tabassam L, Khan MJ, Hussain S, Khattak SA, Shah SK, et al. 2022. Structural, optical and antimicrobial characteristics of ZnO green nanoparticles. *J Sol Gel Sci Technol* 101(2): 401-410. <https://doi.org/10.1007/s10971-022-05726-y>